Robotica: (2021) volume 39, pp. 718–734. © The Author(s), 2020. Published by Cambridge University Press.
doi:10.1017/S0263574720000685

On Motion Planning and Control for Partially Differentially Flat Systems

Yang Bai†*, Mikhail Svinin†, Evgeni Magid‡ and Yujie Wang¶

†*Information Science and Engineering Department, Ritsumeikan University, 1-1-1 Noji-higashi, Kusatsu, Shiga 525-8577, Japan. E-mail: svinin@fc.ritsumei.ac.jp*
‡*Department of Intelligent Robotics, Kazan Federal University, Kremlyovskaya str. 35, Kazan 420008, Russian Federation. E-mail: magid@it.kfu.ru*
¶*Department of Electrical and Computer Engineering, University of Illinois Urbana-Champaign, Urbana-Champaign, IL, USA. E-mail: yujiew4@illinois.edu*

(Accepted June 20, 2020. First published online: July 16, 2020)

SUMMARY
This paper deals with motion planning and control problems for a class of partially differentially flat systems. They possess a feature that the derivative of the fiber variable can be represented purely by the base variable and its derivatives. Based on this feature, a Beta function-based motion planning algorithm is proposed with less computational cost compared with the optimal control formulation while providing similar system performance. Then, an adaptive controller is constructed through a function approximation technique-based approach. Finally, the feasibility of the proposed motion planning and control algorithms is verified by simulations.

KEYWORDS: Motion planning and control; Underactuated systems; Partial differential flatness.

1. Introduction

Underactuated systems have fewer independent actuators than the number of degrees of freedom. In this paper, we focus on a class of partially differentially flat (PDF) systems,[20] a special type of underactuated systems where a portion of configuration variables can be expressed by the derivatives of another portion through integration. The need for analysis and control of this type of systems arises in many practical applications. To realize these applications, two of the important problems need to be solved in the research of underactuated systems: motion planning and control. Typically, the motion planning problem requires to steer the system from an initial state to a given final state and the control problems aim to eliminate the difference between the actual and planned output signals.

Motion planning for an underactuated system requires to generate time trajectories satisfying its nonholonomic constraint.[34] Contrary to the fully actuated systems, it is impossible to find the control input for underactuated ones by directly inverting the system dynamics since they are not square. Instead of the exact inversion, a nilpotent approximation-based technique[23] has been proposed which spans a nilpotent Lie algebra to approximate the original system. However, the motion trajectories generated by this technique may not accurately satisfy the given boundary conditions. Different from approximate techniques, a small amplitude and oscillatory control method[4,12] provides desired trajectories through iteration techniques. However, it is only applicable to Lagrangian systems with controllability rank condition satisfied at low order and the iterations may result to a rather high computational cost. Other than the approximation and iteration techniques, several directions have been explored focusing on the simplification of motion equations. The partial feedback linearization[16] has

* Corresponding author. E-mail: yangbai@fc.ritsumei.ac.jp

been applied for the simplification concerns by removing nonlinearities from the control systems. However, the nonholonomic constraint in the system dynamics, as the core to the motion planning problem, cannot be simplified through this method. The geometric mechanics[5] can also be utilized to simplify an underactuated system by representing it in a kinematic form. Thus, the computational complexity of the motion planning problem is reduced as it is decoupled into path planning followed by time scaling. However, the range of applications for this method is restricted to underactuated systems that are kinematically controllable.

Although the aforementioned motion planning methods work on specific PDF systems such as the cart-pole, they are not applicable to the whole class of systems. The optimal control formulation is generic and feasible for all PDF systems, but it may result to heavy computational cost. In this paper, we develop a generic motion planning method for PDF systems with a rather high speed. This method is based on the concept of fiber and base variables, definitions of which are as follows in ref. [25]. The configuration variables of mechanical systems include the base variables describing the internal shape changes of the system and the fiber variables representing the system's position and orientation change.

The motion planning algorithm is constructed as follows. First, a Beta function multiplied by a constant parameter is selected as a candidate function for the base variable. Its feasibility for the nonlinear system is then proved by showing that the corresponding fiber variable can satisfy the given boundary conditions. Then the parameter of the Beta function is adjusted such that a desired shift for the fiber variable can be obtained. Under the proposed motion planning algorithm, rest-to-rest trajectories for the configuration variables are generated with less computational cost compared with the optimal control formulation.

In the actual implementation however, an underactuated system may not follow the planned trajectories due to un-modeled disturbances such as friction. To eliminate the effect of the disturbances, control problems for the PDF systems are studied.

In the literature, a number of works on the control of underactuated mechanical systems have been proposed. One of the well-known control methods is the energy shaping technique.[7,11,26,32] However, the energy shaping method only works for systems satisfying the passivity condition, which narrows its range of applications. Another commonly used method is the backstepping method which allows the feedback controller to be designed step by step. However, similar to the energy shaping method, the backstepping is applicable to a limited class of systems that are in the backstepping form. Also, when the degree of freedom (DOF) of underactuated systems increases, the procedure of backstepping becomes complicated, and implementation of such a control design on actual systems becomes impractical. Different from the above two methods, the partial feedback linearization[17,18,29] is a generic method, providing a natural global change of coordinates that transforms underactuated systems into the strict feedback form. However, one drawback of this technique is that it requires full knowledge of the system model, which is unrealistic for the practical application when system uncertainties exist. To deal with the uncertainties in system models, the sliding mode control,[8,13,15,19,24,33] a robust control method which depends on switching, can be adopted. This methods, however, is suitable only for small uncertainties. Soft computing methods are more suitable for rather large uncertainties, but the stability is difficult to be proved.

To address both the stability and the adaptiveness, in this paper, we propose an function approximation technique (FAT)-based method inspired by its application to adaptive control problems.[2,3,6,10,30,31] It is model-free, and thus feasible for a wide class of systems and robust to uncertainties. On the other hand, compared with the soft computing techniques, the stability of the FAT-based method can be proved.

The key to the construction of the FAT-based controller is to express an underactuated system by the combination of an approximated square system, referring to the auxiliary system, and a variation term from the original system. This variation term is treated as a time-varying uncertainty to the restructured square system. Then, we parameterize the uncertainty term with a set of chosen basis functions weighted by unknown parameters. These parameters are required to be constants in order to allow the application of the Lyapunov function-based design. Finally, define update laws such that the parameters of the weighted basis functions can be automatically determined and the variation between the auxiliary square system and the original non-square system can be eliminated. By combining these two parts, we obtain a feedback controller that makes the underactuated system asymptotically stable.

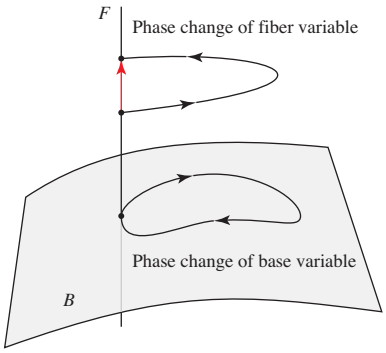

Fig. 1. A closed loop in shape variables producing a displacement in the fiber variable.

The rest of the paper is organized as follows. In Section 2, a rest-to-rest motion planning problem for PDF systems is studied and a Beta function-based algorithm is proposed. In Section 3, the control problem for PDF systems is stated and a corresponding FAT-based algorithm is constructed. In Section 4, the proposed motion planning and control algorithms are verified under simulations for two types of PDF systems, the cart-pole system and the planar ballbot system.[14] Finally, conclusions are drawn in Section 5.

2. Beta function-based motion planning

A PDF system is defined as follows in ref. [20]. A system $\dot{\boldsymbol{x}} = \boldsymbol{F}(\boldsymbol{x}, \boldsymbol{u})$ is PDF if there exists a partition of the states, $\boldsymbol{x} = (\boldsymbol{s}, \boldsymbol{r})$ and outputs $\boldsymbol{y} = \boldsymbol{y}(\boldsymbol{s}, \boldsymbol{u}, \dot{\boldsymbol{u}}, ..., \boldsymbol{u}^{(p)})$ such that $\boldsymbol{s}$ and $\boldsymbol{u}$ can be expressed as functions of $\boldsymbol{y}$ and its derivatives, respectively, and the $\boldsymbol{r}$-state dynamics are that of one or more chains of integrators. Roughly speaking, a system is PDF if we can find a set of outputs and a state partition, such that the inputs and a partition of the states can be obtained from the outputs and their higher-order derivatives without integration.

Without loss of generality, we construct motion planning algorithms for 2DOF PDF systems,[20] which correspond to the shape accelerated systems including the cart-pole system, the hoop-pendulum system, the planar ballbot system and the segway, etc. The motion equations of these systems with one input τ are

$$\begin{bmatrix} m_{ff} & m_{fb} \\ m_{bf} & m_{bb} \end{bmatrix} \begin{bmatrix} \ddot{q}_f \\ \ddot{q}_b \end{bmatrix} + \begin{bmatrix} h_f \\ h_b \end{bmatrix} = \begin{bmatrix} 0 \\ 1 \end{bmatrix} \tau, \tag{1}$$

where $\boldsymbol{q} = (q_f, q_b)$ is the vector for the generalized coordinates and q_f, q_b are, respectively, the fiber and the base variables. The base variable describes the internal shape changes of the system, and the fiber variable represents the system's position and orientation change. As (1) is PDF, the base variable q_b can be taken as the flat output, the second-order derivative of the fiber variable q_f can be expressed purely by τ, q_b, and its derivatives as

$$\ddot{q}_f = h(q_b, \dot{q}_b, \tau). \tag{2}$$

Note that the underactuated portion of the motion equations (first line of (1)) forms a nonholonomic constraint. For systems with nonholonomic constraint, a closed loop phase change of the base variable can lead to a non-zero phase change of the fiber variable, as illustrated in Fig. 1. In this figure, F is the set of fiber variables and the B is the manifold for the base space. A trivial principle fiber bundle with B and F consists of the configuration manifold $Q = B \times F$ to which $\boldsymbol{q}$ belongs.[9]

This property implies that a periodic internal shape change of underactuated system steers its position and orientation. Therefore, one can select the base variable q_b to be the input in the motion planning problem. The selection of q_b as input is implemented by the partial feedback linearization for (1) with respect to q_b conducted below. Selecting

$$\tau = (m_{bb} - m_{bf} m_{ff}^{-1} m_{fb}) u + (h_b - m_{bf} m_{ff}^{-1} h_f), \tag{3}$$

and substituting (3) back into (1) gives

$$\ddot{q}_f = -m_{ff}^{-1} h_f - m_{ff}^{-1} m_{fb} u, \tag{4}$$

$$\ddot{q}_b = u, \tag{5}$$

where u is the auxiliary input. By choosing a state vector $\boldsymbol{x} = (q_f, \dot{q}_f, q_b, \dot{q}_b)$, the partially linearized system (4) and (5) can be written in the state space form as

$$\dot{\boldsymbol{x}} = \boldsymbol{f}(\boldsymbol{x}) + \boldsymbol{G}(\boldsymbol{x})\boldsymbol{u} = \begin{bmatrix} \dot{q}_f \\ -m_{ff}^{-1} h_f \\ \dot{q}_b \\ 0 \end{bmatrix} + \begin{bmatrix} 0 \\ -m_{ff}^{-1} m_{fb} \\ 0 \\ 1 \end{bmatrix} u. \tag{6}$$

2.1. Special feature of PDF systems

A notable property of (6) is that the controllable canonical form of the linearized system of (6) around $q_b = 0$ and $\dot{q}_b = 0$ is an integrator. This property is proved as follows. The linearization of (6) around $q_b = \dot{q}_b = 0$ is expressed as

$$\dot{\boldsymbol{x}} = \boldsymbol{A}\boldsymbol{x} + \boldsymbol{b}u = \begin{bmatrix} 0 & 1 & 0 & 0 \\ 0 & 0 & a_{23} & a_{24} \\ 0 & 0 & 0 & 1 \\ 0 & 0 & 0 & 0 \end{bmatrix} \boldsymbol{x} + \begin{bmatrix} 0 \\ b \\ 0 \\ 1 \end{bmatrix} u, \tag{7}$$

where a_{23}, a_{24}, b are constants. According to (2), the second row of matrix $\boldsymbol{A}$ has two non-zero items a_{23} and a_{24} due to that $\ddot{q}_f$ contains no q_f or $\dot{q}_f$ terms.

To transform the linearized model (7) to the controllable canonical form, one defines a transformation matrix $\boldsymbol{P}$ by

$$\boldsymbol{P} = \begin{bmatrix} \boldsymbol{A}^3\boldsymbol{b} & \boldsymbol{A}^2\boldsymbol{b} & \boldsymbol{A}\boldsymbol{b} & \boldsymbol{b} \end{bmatrix}. \tag{8}$$

By setting $\boldsymbol{x} = \boldsymbol{P}\hat{\boldsymbol{x}}$, one obtains the controllable canonical form of (6) as

$$\dot{\hat{\boldsymbol{x}}} = \boldsymbol{P}^{-1}\boldsymbol{A}\boldsymbol{P}\boldsymbol{x} + \boldsymbol{P}^{-1}\boldsymbol{b}u = \hat{\boldsymbol{A}}\hat{\boldsymbol{x}} + \hat{\boldsymbol{b}}u = \begin{bmatrix} 0 & 1 & 0 & 0 \\ 0 & 0 & 1 & 0 \\ 0 & 0 & 0 & 1 \\ 0 & 0 & 0 & 0 \end{bmatrix} \hat{\boldsymbol{x}} + \begin{bmatrix} 0 \\ 0 \\ 0 \\ 1 \end{bmatrix} u, \tag{9}$$

which is a fourth-order integrator. The analytical solution to the linear system (9) under the minimum effort optimal control problem (the optimal criterion is $\frac{1}{2}\int u^2 \mathrm{d}t$) is well established in the control literature, which is represented as

$$\boldsymbol{x}(t) = e^{\hat{\boldsymbol{A}}t}\left(\left(\boldsymbol{I} - \boldsymbol{W}(t)\boldsymbol{W}(T)^{-1}\right)\boldsymbol{x}(0) + \boldsymbol{W}(t)\boldsymbol{W}(T)^{-1}e^{-\hat{\boldsymbol{A}}T}\boldsymbol{x}(T)\right), \tag{10}$$

where $\boldsymbol{W}(t) = \int_0^t e^{-\hat{\boldsymbol{A}}s}\hat{\boldsymbol{b}}\hat{\boldsymbol{b}}^\top e^{-\hat{\boldsymbol{A}}^\top s}\,\mathrm{d}s$ and T is the total time interval. For a rest-to-rest motion, $e^{-\hat{\boldsymbol{A}}T}\hat{\boldsymbol{x}}(T) = \hat{\boldsymbol{x}}(T)$. Setting the nominal time $\hat{t} = t/T$ and with binomial expansion for $(1-\hat{t})^3$, one obtains

$$q_f^{\text{linear}}(\hat{t}) = \frac{\int_0^T p^3(1-p)^3\mathrm{d}p}{B(4,4)} = \frac{B(\hat{t};4,4)}{B(4,4)},\ q_b^{\text{linear}}(\hat{t}) = \ddot{q}_f^{\text{linear}}(\hat{t}), \tag{11}$$

for the fourth-order integrator, where $B(\hat{t};4,4)$ is the regularized incomplete Beta function. In what follows, as we deal with the fourth-order systems only, $B(\hat{t};4,4)$ will be written as $B(\hat{t})$ unless otherwise specified. The linearized solution for the base variable $q_b^{\text{linear}}(\hat{t})$, which is a polynomial, is later on shown to be a feasible solution to the original nonlinear system (6).

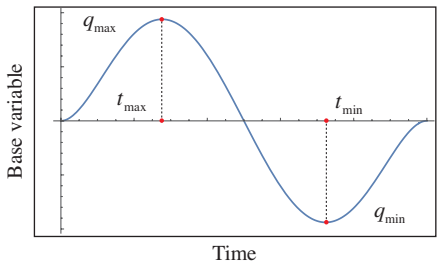

Fig. 2. Motion pattern of the base variable $q_b(t)$

2.2. A Beta function-based motion planner design for a rest-to-rest problem

Based on (6), a rest-to-rest motion planning problem is stated as defining u such that the corresponding trajectories for the state $\boldsymbol{x}$ satisfy the given boundary conditions

$$\begin{aligned}\boldsymbol{x}(0) &= (q_f(0), \dot{q}_f(0), q_b(0), \dot{q}_b(0)) = (0, 0, 0, 0),\\ \boldsymbol{x}(T) &= (q_f(T), \dot{q}_f(T), q_b(T), \dot{q}_b(T)) = (q_{\text{des}}, 0, 0, 0).\end{aligned} \tag{12}$$

The nonlinear optimal control formulation provides a generic way to plan the rest-to-rest motion for system (6). However, it comes with a high computational cost and the algebraic relation between the configuration variables is not analytically known. In this section, we propose a systematic way for capturing the optimal motion pattern by a polynomial function that satisfies the given boundary conditions. The resulting motion planner is less computationally expensive and thus more suitable for real-time application.

The construction of the motion planning algorithm consists of two steps: first one defines a feasible base variable $q_b(t)$ and then computes the corresponding fiber variable $q_f(t)$ under given boundary conditions.

2.2.1. Define the base variable q_b. To construct a less computational expensive but feasible motion planner for system (6) satisfying the rest-to-rest boundary conditions (12), we select

$$q_b(t) = q_b^{\text{linear}}(\hat{t})\Big|_{\hat{t}=t}. \tag{13}$$

Note that $q_b(t)$, as shown in Fig. 2, is an odd function with respect to the middle point, where $t = T/2$. It implies $|q_{\max}| = |q_{\min}|$, where $q_{\max}$ and $q_{\min}$ are constants indicating the maximum and minimum values of $q_b(t)$. Then, we prove its feasibility by showing that the corresponding trajectories of $\boldsymbol{x}(t)$ satisfy the given boundary conditions.

For the sake of simplicity, we represent $q_b(t)$ in the form of a polynomial whose maximum value is 1, weighted by $q_{\max}$. One way to do so is to find the location $t_{\max}$ of the maximum point, calculating the corresponding value $q_b(t_{\max})$, and rendering it to 1. Note the zero-velocity points of $q_b(t)$ are found at $t = 0$, $t = t_{\max}$, $t = t_{\min}$, and $t = T$, where

$$t_{\max} = \left(\frac{5-\sqrt{5}}{10}\right) T, \;\; t_{\min} = \left(\frac{5+\sqrt{5}}{10}\right) T. \tag{14}$$

Thus, the value of $q_{\max} = q_b(t_{\max})$ can be easily calculated and the base variable $q_b(t)$ can be expressed as

$$q_b(t) = q_{\max}\left(\frac{25\sqrt{5}t^2(t-T)^2(2t-T)}{T^5}\right). \tag{15}$$

Having defined the base variable $q_b(t)$ as (15), the auxiliary input $u(t)$ is calculated as the second-order derivative of $q_b(t)$.

Then, one proves that (15) is a feasible candidate function for the base variable $q_b(t)$ to realize a rest-to-rest motion for the original nonlinear underactuated system. As $q_b(t)$, selected as (15),

satisfies the given boundary conditions (12), to prove the feasibility of $q_b(t)$ is equivalent to prove that the corresponding $q_f(t)$ satisfies (12).

As for the PDF systems, the derivative of the fiber variable q_f can be expressed by the derivatives of the base variable q_b, one has

$$\ddot{q}_f = h(q_b, \dot{q}_b). \tag{16}$$

The substitution of the expression of q_b as (15) into (16) gives

$$\ddot{q}_f = h(q_{\max}, t). \tag{17}$$

One can obtain $q_f(t)$ by solving (17) with $q_f(0) = \dot{q}_f(0) = 0$ in (12). Therefore, the initial conditions for q_f are satisfied.

However, the selection of q_b as (15) is considered to be feasible only when the final rest conditions of q_f are also as desired, namely $q_f(T) = q_{\text{des}}$ and $\dot{q}_f(T) = 0$ as given in (12). The final displacement $q_f(T) = q_{\text{des}}$ can be obtained by developing an algorithm for the automatic adjustment of parameter $q_{\max}$, which is shown later on in Section 2.2.2. The proof of the final velocity $\dot{q}_f(T) = 0$ is sketched as follows.

Note that $q_b(t)$ is the second derivative of Beta function, and Beta function has the property that $B(t) = B(T) - B(T - t)$. Therefore, all its even derivatives are odd (asymmetric) and odd derivatives are even (symmetric) with respect to the middle point $t = T/2$. By introducing the new time coordinate $\tilde{t} = t - T/2$, one obtains

$$q_b(\tilde{t}) = q_b\left(t - \frac{T}{2}\right), \ \dot{q}_b(\tilde{t}) = \dot{q}_b\left(t - \frac{T}{2}\right),$$

and thus

$$q_b(-\tilde{t}) = -q_b(\tilde{t}), \ \dot{q}_b(-\tilde{t}) = \dot{q}_b(\tilde{t}). \tag{18}$$

By substituting (18) into (16), one obtains the second derivative of the fiber variable $\ddot{q}_f$ as a function of $\tilde{t}$. If

$$\ddot{q}_f(-\tilde{t}) = -\ddot{q}_f(\tilde{t}), \tag{19}$$

holds, which implies that $\ddot{q}_f(t)$ is odd with respect to $t = T/2$, one obtains that with the initial condition $\dot{q}_f(0) = 0$,

$$\int_0^T \ddot{q}_f(t)\, \mathrm{d}t = \dot{q}_f(T) - \dot{q}_f(0) = 0, \tag{20}$$

which leads to the conclusion that $\dot{q}_f(T) = 0$. Therefore, the selected $q_b(t)$ is a feasible candidate for the rest-to-rest motion planning for the underactuated system (6).

It is important to notice that the Beta function-based algorithm works only when (19) holds. Although a proof of (19) for all PDF systems is yet to be proposed, one can show its validity for typical PDF systems such as cart-pole, hoop-pendulum,[1] and planar ballbot system.[20]

2.2.2. Compute the fiber variable q_f. After defining the based variable q_b, one needs to find the corresponding fiber variable q_f as (15) satisfying given boundary conditions. The fiber variable q_f can be obtained by solving (17) with the rest-to-rest boundary conditions $q_f(0) = \dot{q}_f(0) = \dot{q}_f(T) = 0$ and $q_f(T) = q_{\text{des}}$.

Note that if $q_f(0) = \dot{q}_f(0) = 0$, the condition $\dot{q}_f(T) = 0$ is automatically satisfied (proved in Section 2.2.1). Therefore, one needs to solve (17) with independent boundary conditions

$$q_f(0) = 0, \ \dot{q}_f(0) = 0, \ q_f(T) = q_{\text{des}}. \tag{21}$$

However, one second-order differential equation can only carry two independent boundary conditions. To deal with this problem, one can treat $q_{\max}$ as an independent variable. As $q_{\max}$ is constant, one supplements (17) with one more differential equation[28]

$$\dot{q}_{\max}(t) = 0. \tag{22}$$

Hence, the number of boundary conditions (21), which is three, matches the number of differential equations (a second-order differential Eq. (17) and a first-order differential Eq. (22)). The corresponding boundary value problem is then solvable and solving the boundary value problem is equivalent to solving the rest-to-rest motion planning problem where the value of $q_{\max}$ is automatically determined.

Note that for PDF systems with m degrees of actuation and n degrees of underactuation, the time complexity of an optimal control formulation is $O(4(m+n))$ since it requires to solve $4(m+n)$ first-order differential equations. The Beta function-based method, however, needs to solve only $2m+n$ first-order differential equations. Correspondingly, the time complexity is $O(2m+n)$. Thus, the Beta function-based method has a lower computational cost.

3. FAT-Based Feedback Control

Consider (6) where $\boldsymbol{x} \in \mathbf{R}^m$, $\boldsymbol{u} \in \mathbf{R}^n$ and $m > n$. By selecting the state $\boldsymbol{x}$ to be the system output, the control problem addressed in this paper can be stated as constructing an input $\boldsymbol{u}$ such that $\lim_{t\to\infty} \boldsymbol{x} = \mathbf{0}$. Different from a square system where $\boldsymbol{G}$ is an invertible matrix and a feedback law can be easily formulated, for a non-square system where $\boldsymbol{G}$ is an $m \times n$ matrix, $\boldsymbol{G}^{-1}$ does not exist. The construction of the control law for non-square systems can be conducted as follows.

3.1. Design of controller

To square the control system, one introduces the auxiliary input $\boldsymbol{u}^* \in \mathbf{R}^m$ where

$$\boldsymbol{u} = \boldsymbol{G}^* \boldsymbol{u}^*, \tag{23}$$

and the auxiliary matrix $\boldsymbol{G}^*$ is chosen to be a full rank $n \times m$ matrix. Then, the non-square system (6) is rewritten as

$$\dot{\boldsymbol{x}} = \boldsymbol{f} + \boldsymbol{G}\boldsymbol{G}^* \boldsymbol{u}^*, \tag{24}$$

of which the dimensions for the input and the state are matched. Note that an essential condition for the selection of matrix $\boldsymbol{G}^*$ is that the reconstructed system (24) is required to be controllable, otherwise the design of $\boldsymbol{u}^*$ cannot guarantee the convergence of $\boldsymbol{x}$. Methods for the design of $\boldsymbol{G}^*$ that render system (24) controllable are specified in Appendix.

As matrix $\boldsymbol{G}\boldsymbol{G}^*$ is singular and not invertible, we restructure the system (24) as

$$\dot{\boldsymbol{x}} = \boldsymbol{f} + \boldsymbol{G}\boldsymbol{G}^* \boldsymbol{u}^* + \boldsymbol{u}^* - \boldsymbol{u}^* = \boldsymbol{u}^* + \boldsymbol{d}, \tag{25}$$

where $\boldsymbol{d}(\boldsymbol{x}, \boldsymbol{u}^*, t) = \boldsymbol{f} + (\boldsymbol{G}\boldsymbol{G}^* - \boldsymbol{I})\boldsymbol{u}^*$. Through the above rearrangement, the original non-square system is restructured as the combination of two parts, a square system $\dot{\boldsymbol{x}} = \boldsymbol{u}^*$ referring to the auxiliary system and $\boldsymbol{d}$, which can be viewed as an uncertainty term. Thus, the control problem for the non-square system is reformulated as an adaptive control problem for a square system with time-varying uncertainties, which is stated as constructing $\boldsymbol{u}^*$ such that $\lim_{t\to\infty} \boldsymbol{x} = \mathbf{0}$, with $\boldsymbol{d}$ unknown.

Compared with the adaptive control problem for a system with parametric uncertainty, it is difficult for a system with time-varying uncertainty. Traditional techniques such as the model reference adaptive control (MRAC) are not feasible. To tackle this problem, we adopt the FAT-based adaptive control.[6,10,30,31] Compared with the traditional MRAC, the advantage of the FAT-based control is in the representation of the time-varying uncertainties by a set of given basis functions weighted by a set of unknown constant parameters. Thus, the problem of eliminating the influence of the uncertainty terms is transformed to the estimation of parametric errors. Then, Lyapunov designs are applied to derive proper update laws adjusting the estimates of the unknown parameters. In what follows, the construction of the controller based on the FAT approach is shown in detail.

To control (25), the effect of the uncertainty term $\boldsymbol{d}$ to the system needs to be eliminated. Note that the uncertainty term varies with respect to time t and the state $\boldsymbol{x}$ (the input $\boldsymbol{u}$ can also be expressed by t and $\boldsymbol{x}$). However, at any moment (i.e., $t = 1$, $t = 2$, ...) $\boldsymbol{d}$ is a constant. We use weighted basis functions to approximate $\boldsymbol{d}$ at each moment as

$$\boldsymbol{d}(\boldsymbol{x}, t, \boldsymbol{u}^*) = \sum_{i=0}^{N} \boldsymbol{d}_i \psi_i(\boldsymbol{x}, t) + \boldsymbol{\epsilon}, \tag{26}$$

where $\boldsymbol{d}_i$, referring to the plant parameter, is constant, ψ_i, referring to the basis function, consists of $\boldsymbol{x}$ and t, and $\boldsymbol{\epsilon}$, referring to the approximation error, describes the deviation between the uncertainty $\boldsymbol{d}$ and the weighted basis functions. Hence, by substituting (26) into the state Eq. (25) yields

$$\dot{\boldsymbol{x}} = \boldsymbol{u}^* + \sum_{i=0}^{N} \boldsymbol{d}_i \psi_i(\boldsymbol{x}, t) + \boldsymbol{\epsilon} \tag{27}$$

at each moment.

The control of (27) requires the unknown plant parameters $\boldsymbol{d}_i$ to be identified. To achieve this goal, the plant parameters $\boldsymbol{d}_i$ at each time t are estimated by $\hat{\boldsymbol{d}}_i(t)$, referring to the control parameter. The change of $\hat{\boldsymbol{d}}_i(t)$, with respect to time, is governed by an update law that we are to define in the construction of a feedback controller $\boldsymbol{u}^*$ from the following process.

To construct $\boldsymbol{u}^*$ that steers $\boldsymbol{x}$ to zero and an update law that defines $\hat{\boldsymbol{d}}_i(t)$, a feasible Lyapunov candidate function can be selected

$$V = \frac{1}{2}\boldsymbol{x}^\top \boldsymbol{x} + \frac{1}{2}\sum_{i=0}^{N} \left(\hat{\boldsymbol{d}}_i(t) - \boldsymbol{d}_i\right)^\top \left(\hat{\boldsymbol{d}}_i(t) - \boldsymbol{d}_i\right), \tag{28}$$

which combines both the state $\boldsymbol{x}$ and the estimation error $\hat{\boldsymbol{d}}_i(t) - \boldsymbol{d}_i$ between the plant parameters $\boldsymbol{d}_i$ and their estimates $\hat{\boldsymbol{d}}_i(t)$. Note that the parameters $\boldsymbol{d}_i$ are constants in (28), which implies $\dot{\boldsymbol{d}}_i = \boldsymbol{0}$. Therefore, the derivative of the Lyapunov function candidate is calculated as

$$\dot{V} = \boldsymbol{x}^\top \dot{\boldsymbol{x}} + \sum_{i=0}^{N} \left(\hat{\boldsymbol{d}}_i(t) - \boldsymbol{d}_i\right)^\top \dot{\hat{\boldsymbol{d}}}_i(t). \tag{29}$$

Substituting the vector $\dot{\boldsymbol{x}}$ expressed by (27) into (29) gives

$$\dot{V} = \boldsymbol{x}^\top \left(\boldsymbol{u}^* + \boldsymbol{\epsilon}\right) + \sum_{i=0}^{N} \hat{\boldsymbol{d}}_i(t)^\top \dot{\hat{\boldsymbol{d}}}_i(t) + \sum_{i=0}^{N} \boldsymbol{d}_i^\top \left(\boldsymbol{x}\psi_i(\boldsymbol{x}, t) - \dot{\hat{\boldsymbol{d}}}_i(t)\right).$$

As the control law to be constructed cannot contain unmeasurable elements, the unknown parameters $\boldsymbol{d}_i$ in the derivative of the Lyapunov function need to be excluded. To cancel the terms with $\boldsymbol{d}_i$, define the update law

$$\dot{\hat{\boldsymbol{d}}}_i(t) = \boldsymbol{x}\psi_i(\boldsymbol{x}, t), \tag{30}$$

which leads to

$$\dot{V} = -\boldsymbol{x}^\top \left(\boldsymbol{u}^* + \sum_{i=0}^{N} \hat{\boldsymbol{d}}_i(t)\psi_i(\boldsymbol{x}, t) + \boldsymbol{\epsilon}\right).$$

The approximation error $\boldsymbol{\epsilon}$ needs to be considered in the construction of the auxiliary input $\boldsymbol{u}^*$. To this end, select $\boldsymbol{u}^*$ as

$$\boldsymbol{u}^* = \boldsymbol{u}_x^* + \boldsymbol{u}_\epsilon^*, \tag{31}$$

where $\boldsymbol{u}_\epsilon^*$ is to cover the effect of $\boldsymbol{\epsilon}$. Thus, the derivative of the Lyapunov candidate function $\dot{V}$ becomes

$$\dot{V} = -\boldsymbol{x}^\top \left(\boldsymbol{u}_x^* + \sum_{i=0}^{N} \hat{\boldsymbol{d}}_i(t)\psi_i(\boldsymbol{x}, t)\right) - \boldsymbol{x}^\top \left(\boldsymbol{u}_\epsilon^* + \boldsymbol{\epsilon}\right). \tag{32}$$

Constructing

$$\boldsymbol{u}_x^* = -\boldsymbol{K}\boldsymbol{x} - \sum_{i=0}^{N} \hat{\boldsymbol{d}}_i(t)\psi_i(\boldsymbol{x}, t), \tag{33}$$

where $\boldsymbol{K}$ is a positive matrix, yields

$$\dot{V} = -\boldsymbol{x}^\top \boldsymbol{K}\boldsymbol{x} - \boldsymbol{x}^\top \left(\boldsymbol{u}_\epsilon^* + \boldsymbol{\epsilon}\right). \tag{34}$$

Next, one designs a robust control law for $\boldsymbol{u}_\epsilon^*$ to cover the effect of $\boldsymbol{\epsilon}$. Denote the components of $\boldsymbol{\epsilon} \in \mathbf{R}^m$ to be ϵ_j, where $j = 1, 2, ..., m$. Suppose ϵ_j is bounded and its variation bound is available, that is, there exists $\delta_j > 0$ such that $\|\epsilon_j\| \leq \delta_j$. Then, selecting $\boldsymbol{u}_x^*$ the same as (33) and $u_{\epsilon j}^*$ as

$$u_{\epsilon j}^* = -\delta_j \, \mathrm{sgn}(x_j) \tag{35}$$

yields

$$\dot{V} = -\boldsymbol{x}^\top \boldsymbol{K}\boldsymbol{x} + \sum_{j=0}^{m} \left(x_j \epsilon_j - \delta_j \|x_j\|\right). \tag{36}$$

Note that

$$\sum_{j=0}^{m} \left(x_j \epsilon_j - \delta_j \|x_j\|\right) \leq 0 \tag{37}$$

holds true when ϵ_j is bounded by δ_j. Therefore, $\dot{V} \leq 0$ is guaranteed under the control law

$$\boldsymbol{u} = \boldsymbol{G}^*(\boldsymbol{u}_x^* + \boldsymbol{u}_\epsilon^*). \tag{38}$$

Therefore, the convergence of the state $\boldsymbol{x}$ is achieved while the effect of the approximation error $\boldsymbol{\epsilon}$ is eliminated. Thus, (38) together with the update law (30) formulates the FAT-based controller for non-square systems.

Note that if the number of the basis functions ψ_i is chosen to be sufficiently large such that $\boldsymbol{\epsilon} \approx \mathbf{0}$, the robust term in the designed controller could be dropped while guaranteeing the convergence of the state $\boldsymbol{x}$. Specifically, by selecting $\boldsymbol{u}_\epsilon^* = \mathbf{0}$, the derivative of the Lyapunov function candidate (32) becomes

$$\dot{V} = -\boldsymbol{x}^\top \left(\boldsymbol{u}_x^* + \sum_{i=0}^{N} \hat{\boldsymbol{d}}_i(t)\psi_i(\boldsymbol{x}, t)\right). \tag{39}$$

Constructing the auxiliary input $\boldsymbol{u}^* = \boldsymbol{u}_x^*$ yields

$$\dot{V} = -\boldsymbol{x}^\top \boldsymbol{K}\boldsymbol{x} \leq 0, \tag{40}$$

which implies the convergence of $\boldsymbol{x}$. Hence, the system input $\boldsymbol{u}$ can be simplified from (38) as

$$\boldsymbol{u} = -\boldsymbol{G}^*\left(\boldsymbol{K}\boldsymbol{x} + \sum_{i=0}^{N} \hat{\boldsymbol{d}}_i(t)\psi_i(\boldsymbol{x}, t)\right) \tag{41}$$

with the update law defined by (30).

3.2. Proof of stability

To prove the asymptotic stability of the closed-loop system formulated by (6), (30), and (41) around the equilibrium point, we follow the Lyapunov-like analysis[27] based on the following:

Lemma 1. *If a scalar function V satisfies the following conditions:*

1. *V is lower bounded*
2. *$\dot{V}$ is negative semi-definite*
3. *$\dot{V}$ is uniformly continuous in time*

then $\dot{V} \to 0$ as $t \to \infty$.

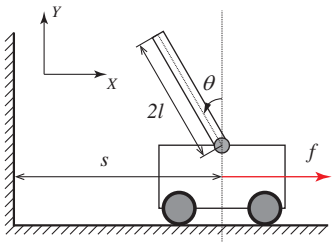

Fig. 3. Cart-pole system.

The Lyapunov function V expressed by (28) satisfies the first and second conditions that V is lower bounded and $\dot{V}$ is negative semi-definite. To follow the Lyapunov-like analysis, we need to show the uniform continuity of $\dot{V}$. This can be done by proving that $\ddot{V}$ is bounded, where

$$\ddot{V} = -2\boldsymbol{x}^\top \boldsymbol{K}\dot{\boldsymbol{x}}. \tag{42}$$

As $\dot{V} \leq 0$, V is bounded and thus so is its component $\boldsymbol{x}$. According to (40), we see that $\dot{V}$ is only composed of variables $\boldsymbol{x}$, $\dot{V}$ is bounded, and, thus, so is its component $\dot{\boldsymbol{x}}$. Therefore, $\ddot{V}$ is bounded since it only contains the elements $\boldsymbol{x}$ and $\dot{\boldsymbol{x}}$ which are shown above to be bounded. Hence, $\dot{V}$ is uniformly continuous. The application of Barbalat's lemma then indicates that $\boldsymbol{x}$ converges to $\mathbf{0}$ when $t \to \infty$.

It should be noted that $\hat{\boldsymbol{d}}_i(t) - \boldsymbol{d}_i$, the error between the parameters and their estimations, is not necessarily asymptotically stable. However, according to (40), we see that the derivative of the Lyapunov function of the closed loop system is negative semi-definite and $\hat{\boldsymbol{d}}_i(t) - \boldsymbol{d}_i$ is bounded, which indicates that the update laws $\hat{\boldsymbol{d}}_i(t)$ finally converge to certain constant values.

4. Case Study

Here, in this section, we provide examples of the proposed motion planning and control algorithms for two PDF systems: the cart-pole system and the planar ballbot system. We choose a fourth-order Beta function in the motion planning examples and a set of polynomial basis functions for estimating the variation $\boldsymbol{d}$ in the control examples, that is, $\psi_i(\boldsymbol{x}, t) = t^i$.

4.1. Cart-pole system

The cart-pole system, as shown in Fig. 3, is a well-known test bed for nonlinear control techniques. It is combined by a sliding cart, on which a inverted pendulum is mounted, connected by a passive pin joint. The displacement of the cart is denoted by s and the pendulum angle by θ, increasing counter-clockwise. The input force f is acting on the cart. The dynamic model of the cart-pole system is obtained[1] as

$$(m + m_p)\ddot{s} - m_p l\cos\theta\ddot{\theta} + m_p l\sin\theta\dot{\theta}^2 = f, \tag{43}$$

$$-m_p l\cos\theta\ddot{s} + J_p\ddot{\theta} + m_p gl\sin\theta = 0, \tag{44}$$

where m, m_p stand for the mass of the cart and of the pendulum and g for the standard gravitational acceleration. Here, one assumes that the pendulum to be a uniform beam of length $2l$. Thus, its inertia momentum with respect to the pin joint $J_p = \frac{1}{12}m_p(2l)^2 + m_p l^2 = \frac{4}{3}m_p l^2$.

Beta function-based motion planning. The rest-to-rest motion planning problem is stated as finding a feasible trajectory for θ such that the corresponding s satisfies the following boundary conditions: $s(0) = 0$, $\dot{s}(0) = 0$, $s(T) = s_{\text{des}}$, $\dot{s}(T) = 0$. The candidate function for the input-based variable θ is chosen in the form (15) with the constant parameter $q_{\max}$ to be determined.

To analyze the performance of the cart-pole system under proposed planner compared with that under nonlinear optimal control formulation seeking for the minimum effort (the optimal criterion is $\frac{1}{2}\int u^2 \mathrm{d}t$), we conduct simulations with respect to various desired shift s_{des} of the fiber variable s. The value of s_{des} changes from 0 to 20π. We plot the configuration variables s and θ as functions of both s_{des} and time t. The motion of the cart-pole system under the Beta function-based planner is shown in Fig. 4 by blue surfaces whereas motion under optimal control in Fig. 5 by red surfaces.

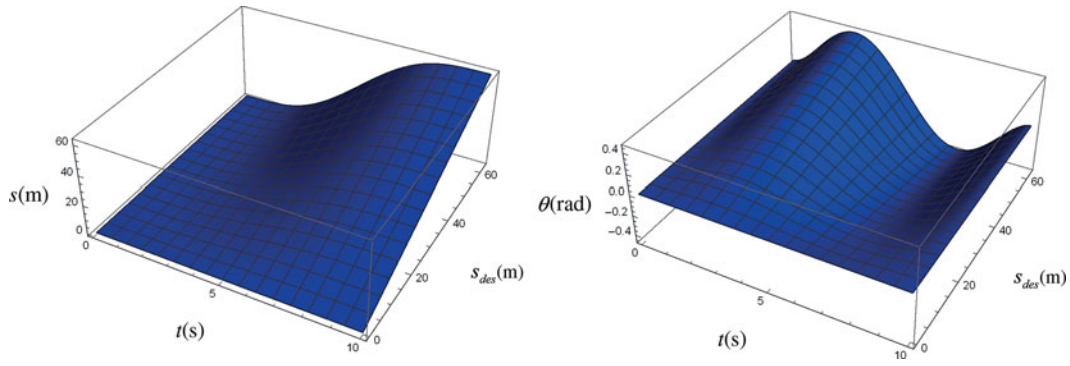

Fig. 4. Motion of the cart-pole system resulted from the Beta function-based control.

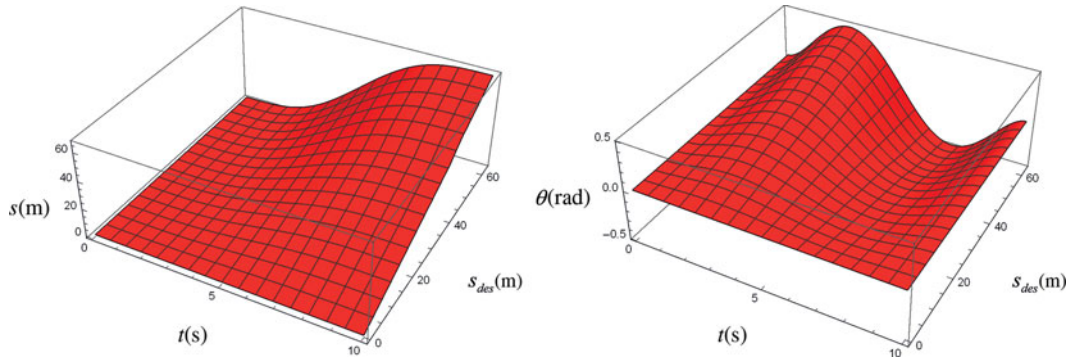

Fig. 5. Motion of the cart-pole system resulted from the minimum effort optimal control.

The numerical values used in the simulation are $m = 1\,\text{kg}$, $m_p = 1\,\text{kg}$, $l = 0.1\,\text{m}$, $g = 9.8\,\text{m/s}^2$, and the time interval $T = 10\,\text{s}$.

By comparing the simulation results of the optimal control and the Beta function-based approach, one finds that the cart motions under both planners are almost the same whereas the pendulum motions differ by less than 0.1 rad in maximum. For both motion planners, the comparison between the values of the cost function J for the cart-pole system is illustrated in Table I. Note that the value of J for the Beta function-based approach is only 0.038% higher than that of the optimal control in maximum, which implies that both motion planners provide similar system performance. Upon this fact, the Beta function-based approach is less computationally expensive and thus more suitable for the real-time applications.

FAT-based control. To apply the constructed control law (41), we select the gain matrix $\boldsymbol{K}$ as diag(5, 5, 5, 5). The initial conditions of the system output are x_1, x_2, x_3, and x_4, and are specified as 2, 0, 0, and 0. The numerical values used in the simulation are $m = 1$ kg, $m_p = 1$ kg, $l = 0.1$ m, $g = 9.8$ m/s^2, and $T = 15$ s. The initial state is (2, 0, 0, 0) and the initial values of the control parameters $\hat{\boldsymbol{d}}_i(t)$ are chosen to be zero.

Under the constructed controller, the system outputs x_1, x_2, x_3, and x_4 converge to zero, as illustrated in Fig. 6. The solid curves stand for the trajectories of the displacement x_1 and velocity x_2 of the cart, whereas the dashed curves for the angular displacement x_3 and angular velocity x_4 of the pendulum.

4.2. Planar ballbot system

The planar ballbot system,[14] illustrated in Fig. 7, is a mobile robot that moves on a rolling hoop. The generalized coordinates of the system are denoted by the hoop angle $\phi(t)$ and the body angle with respect to the ground $\theta(t)$, both of which are increasing counter-clockwise. The red dot on the hoop is its initial contact point to the ground. One revolution of the initial contact point implies a $2\pi R$ linear displacement for the center of the hoop. Note that at the starting configuration ($\phi(0) = 0$), the

Table I. Comparison of the values of the cost function J for the cart-pole system

ϕ_{des}	**Minimum effort optimal control**	**Beta function-based control**
2π	0.00206971	0.00206971
4π	0.00825442	0.00825443
6π	0.0184816	0.0184817
8π	0.0326325	0.0326329
10π	0.0505456	0.0505469
12π	0.0720210	0.0720247
14π	0.0968251	0.0968346
16π	0.124697	0.124718
18π	0.155355	0.155395
20π	0.188503	0.188575

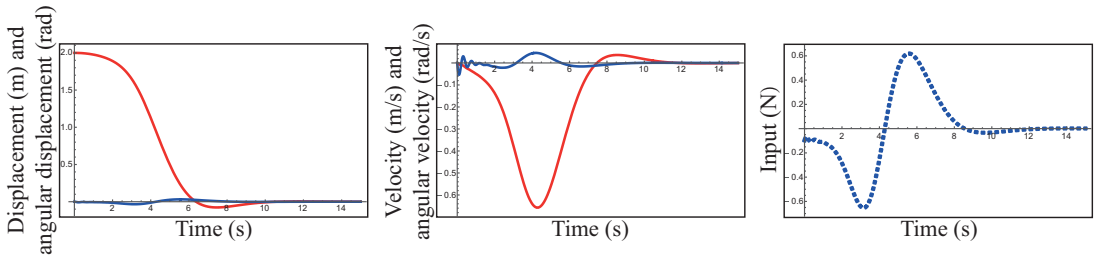

Fig. 6. Motion of the cart-pole system under the FAT-based control.

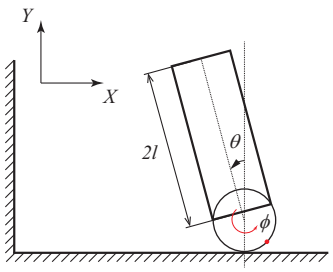

Fig. 7. Planar ballbot system.

initial contact point touches the ground. The input torque τ is acting on the joint between the hoop and the body, also increasing counter-clockwise. The dynamic model is obtained[1] as

$$\left(J_c - m_p Rl\cos\theta\right)\ddot{\phi} + \left(J_p - m_p Rl\cos\theta\right)\ddot{\theta} + m_p l\sin\theta\left(R\dot{\theta}^2 + g\right) = 0, \tag{45}$$

$$-m_p Rl\cos\theta\ddot{\phi} + J_p\ddot{\theta} + m_p gl\sin\theta = \tau, \tag{46}$$

where $J_c = (\frac{4}{3}m + m_p)R^2$. The masses for the hoop and for the body are denoted by m and m_p. R stands for the radius of the hoop and g for the standard gravitational acceleration. Here, one assumes that the body to be a uniform beam of length $2l$. Thus, its inertia momentum with respect to the center of the hoop $J_p = \frac{1}{12}m_p(2l)^2 + m_p l^2 = \frac{4}{3}m_p l^2$.

Beta function-based motion planning. The rest-to-rest motion planning problem is stated as finding a feasible trajectory for θ such that the corresponding ϕ satisfies the following boundary conditions: $\phi(0) = 0$, $\dot{\phi}(0) = 0$, $\phi(T) = \phi_{\text{des}}$, $\dot{\phi}(T) = 0$.

The performance of the ballbot system, under the proposed planner and the optimal control (with the optimal criterion $\frac{1}{2}\int u^2\ \text{dt}$), is compared as follows. We conduct simulations with respect to various desired shift ϕ_{des} of the fiber variable ϕ. The value of ϕ_{des} changes from 0 to 20π. We plot the configuration variables ϕ and θ as functions of both ϕ_{des} and time t. Motion under the Beta function

Table II. Comparison of the values of the cost function J for the planar ballbot system

ϕ_{des}	**Minimum effort optimal control**	**Beta function-based control**
2π	0.00029573	0.00029573
4π	0.0011836	0.0011836
6π	0.00266544	0.00266544
8π	0.00474466	0.00474466
10π	0.00742581	0.00742582
12π	0.0107149	0.0107149
14π	0.0146193	0.0146194
16π	0.0191479	0.0191480
18π	0.0243110	0.0243113
20π	0.0301207	0.0301211

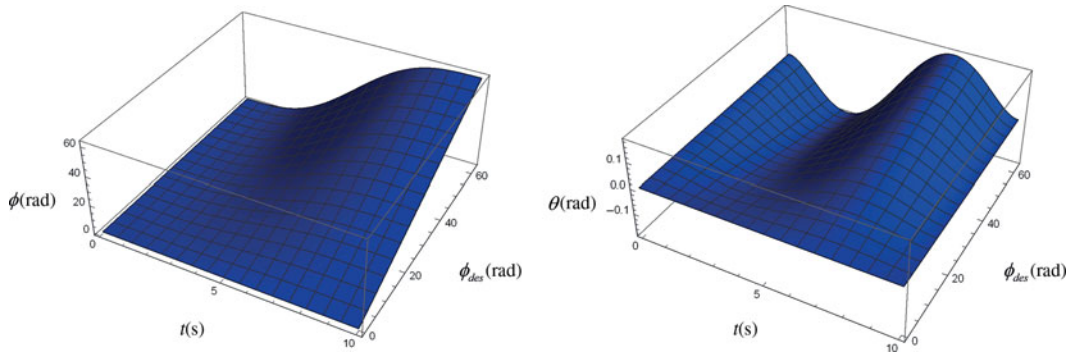

Fig. 8. Motion of the planar ballbot system resulted from the Beta function-based control.

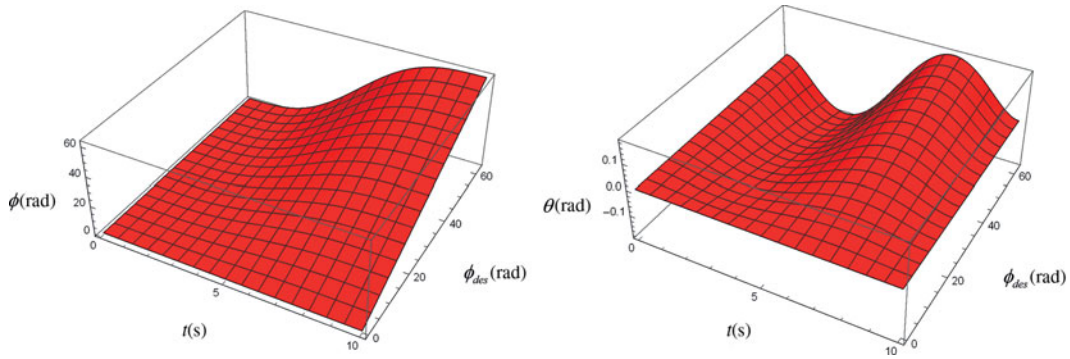

Fig. 9. Motion of the planar ballbot system resulted from the minimum effort optimal control.

based planner is shown in Fig. 8 by blue surfaces, whereas motion under optimal control in Fig. 9 by red surfaces. The numerical values used in the simulation are $m = 2\,\text{kg}$, $m_p = 1\,\text{kg}$, $R = 0.2\,\text{m}$, $l = 0.3\,\text{m}$, $g = 9.8\,\text{m/s}^2$, and the time interval $T = 10\,\text{s}$.

Similar to the cart-pole system, for the planar ballbot system, the hoop motions resulted from the optimal control and the Beta function approach are almost the same whereas the body motions differ by less than 0.2 rad in maximum. The comparison between the values of the cost function J for the planar ballbot system under both motion planners is illustrated in Table II. Note that the value of J for the Beta function-based approach is only 0.0013% higher than that of the optimal control in maximum, which implies that both motion planners provide similar system performance. Upon this fact, the less computationally expensive Beta function-based method is more suitable for the real-time applications.

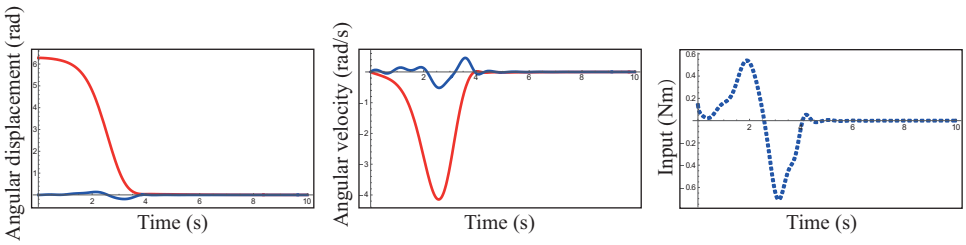

Fig. 10. Motion of the planar ballbot system under the FAT-based control.

FAT-based control. In this section, we test the control law (38) also on the planar ballbot system. The numerical values used in the simulation are selected the same as in the motion planning example. The initial conditions of the system output x_1, x_2, x_3, and x_4 are specified as 2π, 0, 0, and 0, and the initial values of the control parameters $\hat{\boldsymbol{d}}_i(t)$ are chosen to be zero. The gain matrix $\boldsymbol{K}$ is selected as diag(1, 25, 5, 5).

Under the constructed controller, the system outputs x_1, x_2, x_3, and x_4 converge to zero, as illustrated in Fig. 10. The red solid curves stand for the trajectories of the displacement x_1 and velocity x_2 of the hoop, whereas the blue solid curves for the angular displacement x_3 and angular velocity x_4 of the body. The input signal is illustrated by the dashed curve.

5. Conclusions

Motion planning and control problems for a class of PDF systems have been considered in this paper. A Beta function-based motion planning algorithm has been constructed. The second-order derivative of Beta function multiplied by a constant parameter was selected as a candidate for the base variable. The parameter can be adjusted such that a desired shift for the fiber variable is obtained. Under the proposed motion planning algorithm, rest-to-rest motion trajectories for the configuration variables were generated with similar system performance but less computational cost, compared with the nonlinear optimal control formulation.

To guarantee that the actual motions of systems converge to the planned trajectories, a FAT-based control algorithm was proposed. By introducing an auxiliary input, an underactuated system was restructured as the combination of a fully actuated system and the variation from the original system. In the control process, the variation term was replaced by its approximation as a chosen basis function weighted by constant parameters to be determined. These unknown plant parameters were estimated at each instant, denoted by the adjustable control parameters using a defined update law. Thus, the influence to the control process caused by the variation term can be eliminated.

The feasibility of the Beta function-based motion planner (satisfaction of given boundary conditions) has been proved, and the stability of the FAT-based control method has been established. The proposed motion planning and control techniques have been verified under simulations for two types of PDF system, the cart-pole system and the planar ballbot. In the future work, more types of underactuated systems will be tested under the proposed techniques to extend their range of application. Moreover, experimental works will be conducted for validating the proposed algorithms in practice.

6. Discussions

For the proposed motion planning, there are also several points to be improved in the future work. For the Beta function-based algorithm, the partial feedback linearization with respect to the base variable q_b may induce an algorithmic singularity (e.g., $\theta = \pi/2$ in the cart-pole system). To deal with the singularity, several methods can be adopted. For example, by adjusting the time interval T, q_b is limited in certain range that does not contain the singular points; by dividing the desired shift of the fiber variable q_{des} into several portions, q_b can be formed by two or more connecting second derivatives of Beta function; or, by selecting a rest-to-rest function for q_b with more than one oscillation, q_{des} can be reached with acceptable amplitudes of q_b away from the singularities.

The FAT-based control method has the following features. Firstly, it is model-free and thus, applicable to a wide range of systems. Secondly, the design of the FAT controller is based on a robust

adaptive approach and therefore can reject the effect of the system uncertainties or external disturbances to the control system. Thirdly, unlike other model-free methods such as the soft computing techniques, the stability for systems under the FAT control has been well established. The following issues need to be clarified for the control algorithms in the future research. Firstly, a unified way of selecting $\boldsymbol{G}^*$ needs to be developed. Secondly, we chose the polynomials for estimating the variation term $\boldsymbol{d}$. However, the advantages and disadvantages for this type of basis function are not analyzed and more candidates need to be investigated.

Acknowledgements

This work was supported in part by the Japan Science and Technology Agency, through the JST Strategic International Collaborative Research Program under Project 18065977, and in part by the Russian Foundation for Basic Research under Project 19-58-70002.

References

1. Y. Bai, M. Svinin and M. Yamamoto, "Motion Planning for a Hoop-Pendulum Type of Underactuated Systems," *Proceedings of the IEEE International Conference on Robotics and Automation* (2016) pp. 2739–2744.
2. Y. Bai, M. Svinin and M. Yamamoto, "Adaptive Trajectory Tracking Control for the Ball-Pendulum System with Time-Varying Uncertainties," *Proceedings of the IEEE/RSJ International Conference on Intelligent Robots and Systems* (2017) pp. 2083–2090.
3. Y. Bai, M. Svinin and M. Yamamoto, "Function approximation based control for non-square systems," *SICE J. Control Measure. Syst. Integr.* **11**(6), 477–485 (2018).
4. F. Bullo, N. E. Leonard and A. D. Lewis, "Controllability and motion algorithms for underactuated Lagrangian systems on lie groups," *IEEE Trans. Autom. Control* **45**(8), 1437–1454 (2000).
5. F. Bullo and K. M. Lynch, "Kinematic controllability for decoupled trajectory planning in underactuated mechanical systems." *IEEE Trans. Robot. Autom.* **17**(4), 402–412 (2001).
6. M. Chien and A. Huang, "Adaptive control for flexible-joint electrically driven robot with time-varying uncertainties," *IEEE Trans. Ind. Electron.* **54**(2), 1032–1038 (2007)
7. B. Gao, X. Zhang, H. Chen and J. Zhao. "Energy-Based Control Design of an Underactuated 2-Dimensional Tora System," *Proceedings of the IEEE/RSJ International Conference on Intelligent Robots and Systems* (2009) pp. 1296–1301.
8. J. Huang, Z. H. Guan, T. Matsuno, T. Fukuda and K. Sekiyama, "Sliding-mode velocity control of mobile-wheeled inverted-pendulum systems," *IEEE Trans. Robot.* **26**(4), 750–758 (2010).
9. S. Kelly and R. Murray, "Geometric phases and robotic locomotion," *J. Robot. Syst.* **12**(6), 417–431 (1995).
10. Y. Liang, S. Cong and W. Shang, "Function approximation-based sliding mode adaptive control," *Nonlinear Dyn.* **54**(3), 223–230 (2008).
11. I. Fantoni and R. Lozano, *Non-Linear Control for Underactuated Mechanical Systems* (Springer-Verlag, New York, NY, USA, 2002).
12. S. Martinez, J. Cortes and F. Bullo, "Analysis and design of oscillatory control systems," *IEEE Trans. Autom. Control* **48**(7), 1164–1177 (2003).
13. L. C. McNinch and H. Ashrafiuon, "Predictive and Sliding Mode Cascade Control for Unmanned Surface Vessels," *Proceedings of the American Control Conference* (2011) pp. 184–189.
14. U. Nagarajan, G. Kantor and R. L. Hollis, "Trajectory Planning and Control of an Underactuated Dynamically Stable Single Spherical Wheeled Mobile Robot," *Proceedings of the IEEE International Conference on Robotics and Automation* (2009) pp. 3743–3748.
15. S. G. Nersesov, H. Ashrafiuon and P. Ghorbanian, "On the Stability of Sliding Mode Control for a Class of Underactuated Nonlinear Systems," *Proceedings of the American Control Conference* (2010) pp. 3446–3451.
16. Z. Neusser and M. Valasek, "Control of the underactuated mechanical systems using natural motion," *Kybernetika* **48**(2), 223–241 (2012).
17. R. Olfati-Saber, "Trajectory Tracking for a Flexible One-Link Robot Using a Nonlinear Noncollocated Output," *Proceedings of the 39th IEEE Conference on Decision and Control* (2000) pp. 4024–4029.
18. K. Y. Pettersen and H. Nijmeijer, "Tracking Control of an Underactuated Surface Vessel," *Proceedings of the 37th IEEE Conference on Decision and Control* (1998) pp. 4561–4566.
19. D. W. Qian, J. Q. Yi and D. B. Zhao, "Robust Control Using Sliding Mode for a Class of Underactuated Systems with Mismatched Uncertainties," *Proceedings of the IEEE International Conference on Robotics and Automation* (2007) pp. 1449–1454.
20. S. Ramasamy, G. Wu and K. Sreenath, "Dynamically Feasible Motion Planning Through Partial Differential Flatness," *Proceedings of Robotics: Science and Systems* (2014) pp. 125–130.
21. J.-M. Coron, *Control and Nonlinearity* (American Mathematical Society, Boston, MA, USA, 2007).
22. Y. Bai, M. Svinin, Y. Wang and E. Magid, "Function Approximation Technique Based Control for a Class of Nonholonomic Systems," *Proceedings of IEEE IEEE/SICE International Symposium on System Integration*, Honolulu, Hawaii, USA, January 2020.

23. C. Romero-Melendez and F. Monroy-Perez, "The motion planning problem: Differential flatness and nilpotent approximation," *Cybern. Phys.* **2**(3), 133–142 (2012).
24. V. Sankaranarayanan and A. D. Mahindrakar, "Control of a class of underactuated mechanical systems using sliding modes," *IEEE Trans. Robot.* **25**(2), 459–467 (2009).
25. E. Shammas, Generalized Motion Planning for Underactuated Mechanical Systems *Ph.D. Thesis* (Carnegie Mellon University, Pittsburgh, Pennsylvania, 2006).
26. A. Shiriaev, H. Ludvigsen, O. Egeland and A. Pogromsky, "On Global Properties of Passivity Based Control of the Inverted Pendulum," *Proceedings of the 38th IEEE Conference on Decision and Control* (1999) pp. 2513–2518.
27. J. E. Slotine and W. Li, *Applied Nonlinear Control* (Prentice Hall International Inc., Englewood Cliffs, New Jersey, 1991).
28. M. Sofronniou and R. Knapp, *Advanced Numerical Differential Equation Solving in Mathematica* (Wolfram Research, Inc., Champaign, IL, 2008).
29. M. W. Spong, "Partial Feedback Linearization of Underactuated Mechanical Systems," *Proceedings of the IEEE/RSJ International Conference on Intelligent Robots and Systems* (1994) pp. 314–321.
30. Y. Tsai and A. Huang, "Fat-based adaptive control for pneumatic servo systems with mismatched uncertainties," *Mech. Syst. Signal Process.* **22**(6), 1263–1273 (2008).
31. F. Tyan and S. Lee, "An Adaptive Control for Rotating Stall and Surge of Jet Engines – A Function Approximation Approach. *Proceedings of the 44th IEEE Conference on Decision and Control, and the European Control Conference 2005* (2005) pp. 5498–5503.
32. X. Xin and M. Kaneda, "Analysis of the energy-based control for swinging up two pendulums," *IEEE Trans. Automat. Contr.* **50**(5), 679–684 (2005).
33. R. Xu and U. Özgüner, "Sliding mode control of a class of underactuated systems," *Automatica* **44**(1), 233–241 (2008).
34. A. Ladd and L. Kavraki, "Motion Planning in the Presence of Drift, Underactuation and Discrete System Changes." *Proceedings of Robotics: Science and Systems (RSS2005)* (2005) pp. 233–240.

Appendix

Methods for the design of $\boldsymbol{G}^*$ that render system (24) controllable are specified as follows. It should be noted that there is no unique way for defining $\boldsymbol{G}^*$ in (23). Depending on the estimation of control systems, it can be selected based on the following considerations.

Firstly, for the control system (6) whose tangent linearization preserves controllability, one can design $\boldsymbol{G}^*$ as follows. The linearization of (6) at the equilibrium $(\boldsymbol{x}_e, \boldsymbol{u}_e)$ gives

$$\dot{\boldsymbol{x}} = \boldsymbol{A}\boldsymbol{x} + \boldsymbol{B}\boldsymbol{u}, \tag{A1}$$

where $\boldsymbol{A} = \frac{\partial(\boldsymbol{f}+\boldsymbol{G}\boldsymbol{u})}{\partial \boldsymbol{x}}\Big|_{\boldsymbol{x}_e,\boldsymbol{u}_e}$, $\boldsymbol{B} = \frac{\partial(\boldsymbol{f}+\boldsymbol{G}\boldsymbol{u})}{\partial \boldsymbol{u}}\Big|_{\boldsymbol{x}_e,\boldsymbol{u}_e}$. One selects $\boldsymbol{G}^*$ in (23) as a constant matrix such that

$$\mathrm{Re}\Big[\lambda\big(\boldsymbol{A}_{m\times m} - \boldsymbol{B}_{m\times n}\boldsymbol{G}^*_{n\times m}\boldsymbol{K}_{m\times m}\big)\Big] < 0, \tag{A2}$$

where $\boldsymbol{K}$ is positive definite. Thus, the closed loop system

$$\dot{\boldsymbol{x}} = (\boldsymbol{A} - \boldsymbol{B}\boldsymbol{G}^*\boldsymbol{K})\boldsymbol{x}, \tag{A3}$$

formulated by the linearized system (A1) and the state feedback portion $\boldsymbol{u} = -\boldsymbol{G}^*\boldsymbol{K}\boldsymbol{x}$ of the FAT-based controller, is stable. The effect of the variation between the linearized system (A1) and the original system (6) can be eliminated by the rest part of the FAT-based controller. Note that the stability of (A3) also indicates the controllability of a linear system

$$\dot{\boldsymbol{x}} = \boldsymbol{A}\boldsymbol{x} + \boldsymbol{B}\boldsymbol{G}^*\boldsymbol{u}^*, \tag{A4}$$

where $\boldsymbol{u}^* \in \mathbb{R}^m$ is viewed as the input. It is because the selection of $\boldsymbol{u}^* = -\boldsymbol{K}\boldsymbol{x}$ renders (A4) to the stable form (A3). As (A4) is the linearized system of (24) at the equilibrium, the controllability of (A4) implies the local controllability of the restructured system (24) at the equilibrium.[21]

Secondly, for control systems whose tangent linearization does not preserve controllability, such as the nonholonomic systems, one may select matrix $\boldsymbol{G}^*$ as the weighted pseudoinverse of $\boldsymbol{G}$ as

$$\boldsymbol{G}^* = (\boldsymbol{G}^\top \boldsymbol{W}\boldsymbol{G})^{-1}\boldsymbol{G}^\top \boldsymbol{W}. \tag{A5}$$

The constant matrix $\boldsymbol{W}$ is designed such that system (24) is controllable. The controllability proof of (24) for typical nonholonomic systems such as the unicycle system and the spherical rolling robot can be found in ref. [22] with the selection of $\boldsymbol{G}^*$ as (A5).

Thirdly, for nonlinear systems (for instance, mechanical systems) modeled by

$$\boldsymbol{M}(\boldsymbol{q})\ddot{\boldsymbol{q}} + \boldsymbol{N}(\boldsymbol{q}, \dot{\boldsymbol{q}}) = \boldsymbol{F}(\boldsymbol{q})\boldsymbol{u}, \tag{A6}$$

the design of $\boldsymbol{G}^*$ can be simplified by introducing, in the spirit of the sliding mode control, the variable $\boldsymbol{x} = \dot{\boldsymbol{q}} + \boldsymbol{\Lambda}\boldsymbol{q}$, where $\boldsymbol{\Lambda}$ is a constant positive-definite Hermite matrix. Note that through this design, when $\boldsymbol{x}$ approaches zero, $\boldsymbol{q}$ converges to zero as well. The derivative of $\boldsymbol{x}$ gives

$$\dot{\boldsymbol{x}} = \ddot{\boldsymbol{q}} + \boldsymbol{\Lambda}\dot{\boldsymbol{q}}. \tag{A7}$$

Rearranging (A6) as $\ddot{\boldsymbol{q}} = -\boldsymbol{M}^{-1}\boldsymbol{N} + \boldsymbol{M}^{-1}\boldsymbol{F}\boldsymbol{u}$ and substituting it into (A7) gives the state equation $\dot{\boldsymbol{x}} = \boldsymbol{f} + \boldsymbol{G}\boldsymbol{u}$, where $\boldsymbol{f} = -\boldsymbol{M}^{-1}\boldsymbol{N} + \boldsymbol{\Lambda}\dot{\boldsymbol{q}}$ and $\boldsymbol{G} = \boldsymbol{M}^{-1}\boldsymbol{F}$. Compared with selecting $(\boldsymbol{q}, \dot{\boldsymbol{q}})$ as the state vector, the dimension of the state equation is halved and thus, the corresponding design of matrix $\boldsymbol{G}^*$ is simplified. Then, $\boldsymbol{G}^*$ can be selected through the two aforementioned methods.